Available online at www.sciencedirect.com
ScienceDirect
International Journal of Heat and Mass Transfer 51 (2008) 1071–1084
International Journal of HEAT and MASS TRANSFER
www.elsevier.com/locate/ijhmt

A new critical heat flux correlation for vertical water flow through multiple thin rectangular channels

C.T. Wright [a,*], J.E. O'Brien [a], R.E. Spall [b]

[a] Idaho National Laboratory, Idaho Falls, ID 83415, USA
[b] Department of Mechanical and Aerospace Engineering, Utah State University, Logan, UT 84322, USA

Received 15 May 2006; received in revised form 23 May 2007
Available online 24 August 2007

Abstract

A critical heat flux (CHF) study of the vertical up-flow of water through multiple thin rectangular channels was conducted. Pressures varied from 89.8 to 115 kPa, inlet temperatures from 291 to 306 K, and mass fluxes from 9.5 to 39 kg m^{-2} s^{-1}. Electrical resistance heaters embedded in aluminum provided a uniform heat flux. A more universal and robust CHF correlation based on the geometry of the Advanced Test Reactor at Idaho National Laboratory was developed. This new CHF correlation predicts 126 data points from this and three previous studies within an error of ±8.5% with a 95% confidence.

Keywords: Critical heat flux; Boiling heat transfer; Nuclear reactor safety; Rectangular flow channels; Multiple flow channels

1. Introduction

A fundamental understanding of flow boiling heat transfer and its potential critical heat flux (CHF) limit is important to the safe and economic operation of high-heat-flux systems such as the Advanced Test Reactor (ATR) in use at Idaho National Laboratory (INL), particularly under accident conditions such as loss-of-coolant or loss-of-flow situations. This understanding is vital in light of the current social-economical demands being applied by an ever-increasing need for abundant and reliable energy. Based on these demands and our current understanding of flow boiling heat transfer, CHF research continues to address the challenge of developing robust data correlations that can be applied to a wide range of accident scenarios where flow conditions, surface materials, and geometric configurations significantly influence the CHF limit of the flow boiling systems.

Previous studies on flow boiling heat transfer through enclosed narrow channels reveal several important operating parameters and geometric factors that significantly affect the CHF condition. Generally, these factors include the flow conditions of the cooling fluid, the type of heated material in the test section, and the number and shape of the heated channels [1–4]. Due to the complex nature of this type of heat transfer, past studies most often focused on a small subset of these factors related to specific applications. Thus, these studies often resulted in CHF correlations that do not include factors applicable to more broad applications. Therefore, it becomes necessary to develop new or modify existing correlations in order to create more robust and universal relationships for use in the design and operation of high-heat-flux energy systems.

Early research on the CHF phenomena, such as those by Bernath [5], and Bergles and Rohsenow [6], examined CHF data related to the mechanisms governing the behavior of boiling systems with the intent of developing a universal CHF correlation. Although these early correlations have not gained acceptance as being universally applicable, some researchers still feel that given the correct dimensionless parameters or experimental constants, a universal correlation could be developed [1,7–12]. Other experimentalists, however, feel that a universal CHF correlation is still far

* Corresponding author. Tel.: +1 208 526 3075; fax: +1 208 526 0690.
E-mail address: christopher.wright@inl.gov (C.T. Wright).

0017-9310/$ - see front matter © 2007 Elsevier Ltd. All rights reserved.
doi:10.1016/j.ijheatmasstransfer.2007.05.013

Nomenclature

A	flow area [m^2] (Eq. (4))
A_h	heated surface area [m^2] (Eq. (5))
Bi	Biot number (Eq. (17))
Bo	Boiling number (Eq. (23))
c_p	specific heat at constant pressure [$J\,kg^{-1}\,K^{-1}$]
D_{hy}	hydraulic-equivalent diameter [m]
g	local acceleration due to gravity [$m\,s^{-2}$]
G	mass flux [$kg\,m^{-2}\,s^{-1}$]
G^*	dimensionless mass flux (Eq. (2))
h	convective heat transfer coefficient [$W\,m^{-2}\,K^{-1}$] (Eq. (22))
h_{fg}	enthalpy of vaporization [$J\,kg^{-1}$]
Δh_i	inlet subcooling enthalpy [$J\,kg^{-1}$] (Eq. (6))
k	thermal conductivity [$W\,m^{-1}\,K^{-1}$]
L	channel length [m]
L_c	characteristic length [m] (Eqs. (18), (24))
L_h	channel heated length [m]
$\dot{m}$	mass flow rate [$kg\,s^{-1}$]
P	static pressure [Pa]
P_h	heated perimeter [m]
P_w	wetted perimeter [m]
q	electric heating power [W]
q''_{chf}	critical heat flux q_{max}/A_h [$W\,m^{-2}$]
q^*	dimensionless critical heat flux (Eq. (1))
s	channel gap [m]
T	temperature [K]
V	volume [m^3]
w	channel width [m]
w_h	channel heated width [m]
We_D^{-1}	inverse Weber number based on hydraulic-equivalent diameter (Eq. (16))
We_L^{-1}	inverse Weber number based on channel length (Eq. (7))

Greek symbols

λ	Taylor wavelength [m] (Eq. (3))
v	kinematic viscosity [$m^2\,s^{-1}$]
ρ	mass density [$kg\,m^{-3}$]
$\Delta\rho$	liquid–vapor density difference [$kg\,m^{-3}$]
σ	surface tension [$N\,m^{-1}$]

Subscripts

f	fluid
g	vapor
i	inlet
m	metal
sat	saturation

off and choose to focus on developing correlations based on specific test parameters such as flow direction, number of heated channels, heated surface material, and flow channel geometry.

Croft [13] and Waters [14] presented two early studies on effects of flow direction on CHF. Their research showed that CHF values are lower for down-flow as opposed to up-flow due to instabilities caused by the counter-current flow of liquid and vapor near the channel exit. Subsequent studies quantified the CHF values from down-flow to range between 10% and 30% lower than the up-flow values for similar flow conditions [15–18]. Sudo et al. [19,20] and Sudo and Kaminaga [21] defined three flow regions representing low ($<\sim30\,kg\,m^{-2}\,s^{-1}$), medium ($\sim30$–$1000\,kg\,m^{-2}\,s^{-1}$), and high ($>\sim1000\,kg\,m^{-2}\,s^{-1}$) mass fluxes that affect CHF values for up- and down-flow conditions. Their results indicate that, for defined low-mass fluxes, the CHF values for up- and down-flow conditions are the same. For defined medium mass flux values, a significant decrease in CHF occurs for down-flow when compared to up-flow under similar conditions. Finally, for defined high-mass flux region, no significant differences between up- and down-flow CHF were observed, suggesting the buoyancy effects on the system are no longer as important as the forced flow of the fluid. Thus, studies that neglect the effects of buoyancy on CHF "are justified in doing so only when the velocities are high" [1].

In addition, Ambrosek and Durney [22] revealed that the material used to fabricate the channels had a significant effect on the overall heat transfer characteristics and CHF values. They suggest that aluminum–water systems have CHF values on the order of 20% higher than those measured for stainless steel. This result supports a pool boiling study by Tachibana et al. [23] in which several different surface materials including stainless steel, aluminum, nickel, and copper were tested. Results indicated that the aluminum-heated surface had about 25% higher CHF values than did the stainless steel surface under equivalent conditions. Additional studies supporting the conclusion that heated aluminum surfaces support higher CHF values when compared to stainless steel attributes the difference to aluminum's higher heat conducting properties [1,24].

Similar to the instabilities identified in flow-direction studies, Murase et al. [25] and Suzuki et al. [26] noted that down-flow CHF in multiple-channel systems was reached due to competing channel-to-channel flows. Boure et al. [27] suggested that the mechanisms behind competing flows between single- and multiple-channel systems, such as the redistribution of fluid among parallel channels, induces two different types of flow instabilities, namely channel (multi-channel effect) and system (flow direction effect). Though these mechanisms have not been thoroughly investigated, several studies have quantified the effects of down-flow instabilities in both single and multiple channels

systems [18,28,29]. In fact, O'Brien and Stoots [29] concluded that under upflow conditions flow instabilities had little effect on the CHF of the system showing comparable data between their multiple-channel configuration and Oh and Englert's single channel configuration. Nevertheless, more CHF studies are needed to sufficiently quantify channel and system instabilities with respect to single- versus multiple-channel systems.

Other parameters, such as the cross-sectional geometry of the test sections, have also shown a substantial effect on CHF values. Round and rectangular cross-sections have made up the two primary divisions in geometrically influenced CHF data. Concerned that a correlation based on multiple channel geometries did not accurately predict CHF in the ATR, Pagh [4] compiled a database containing only annular geometry and used it to develop a new CHF correlation. A comparison to the Groeneveld Lookup Table [7] showed the lookup table to be more conservative in all cases, while Pagh's [4] correlation predicted roughly the same value as other independent annular CHF correlations.

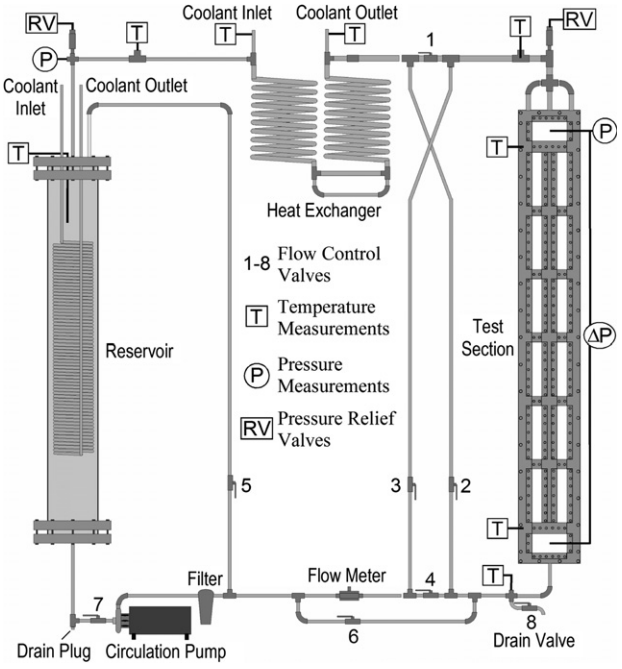

Fig. 1. Flow loop schematic.

It is clear from the results of past CHF studies that different flow parameters and heated channel geometries can significantly affect a system's CHF characteristics. Thus, the main purpose of this study was to investigate the CHF limit of flow boiling heat transfer as it relates to the vertical flow of water through multiple rectangular aluminum channels with side-vent cross-flow to better quantify these specific parameters. The measured CHF data was used to develop a new CHF correlation that addresses many concerns, including flow direction, number of heated channels, heated surface material, and flow channel geometry variables.

2. Experimental apparatus

The experimental study was conducted in a closed-loop flow system depicted schematically in Fig. 1. The major components of the flow loop include the heated test section, the heat exchanger, the cooling fluid reservoir, the circulation pump, the particulate filter, the paddle-wheel-type flow meter, and the connecting pipes, fittings, and valves. The physical arrangement of each component allows demineralized water to flow both upward and downward through the test section. Two bypass lines provide active control over the hydrodynamic characteristics of the test section by creating "stiff" or "soft" flow conditions through the test section, which have an effect on the overall behavior of CHF [16]. They also serve as a means of cleaning and degassing the test section before test runs.

The multiple-channel test section is made from type 6064-T6 aluminum and includes four primary flow channels (50.8 mm × 1.0 mm × 1.27 m), three secondary side channels (25.4 mm × 1.3 mm × 1.27 m), and six side vents, allowing horizontal mass flux communication between the flow channels. All flow channels are vertically oriented and share common upper and lower plenums. One long side of each primary flow channel is formed from an electrically heated aluminum substrate. Four embedded heaters with a maximum power output of 36 kW (9 kW per heater) provide a uniform heat flux over the length of the flow channels. A cross-sectional view of the test section shows the four primary flow channels, the three side-flow channels, the four FIREBAR® heaters, and other structural fasteners

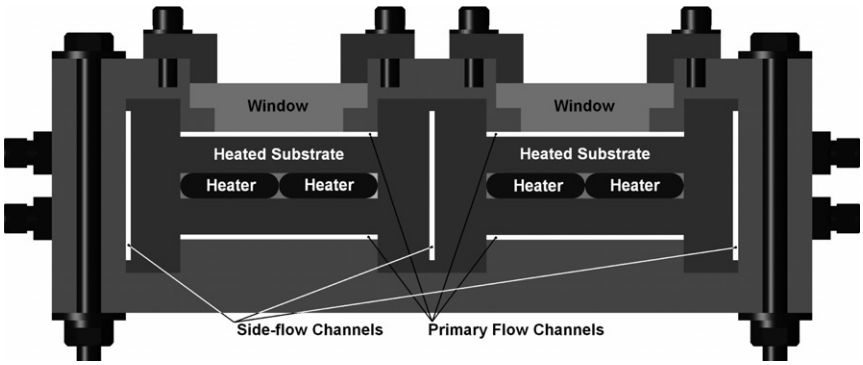

Fig. 2. Cross-sectional view of the test section showing the flow channels, the heated subtrate and embedded heaters, and the viewing windows.

and components (see Fig. 2). Additional slots connect the side flow and main flow channels at axial locations represented with a dotted black line in Fig. 2.

The flow conditions and input power to the test section are monitored and recorded with absolute and differential pressure transducers, type K thermocouples, watt transducers, and a data acquisition system. The pressure transducers were located at the inlet and outlet of the test section and at the top of the reservoir. The thermocouples were positioned every 50 mm along the test section and at various locations around the flow loop. The watt transducers were inline with the two power leads connected to the FIREBAR® heaters. Signals from each of the components were acquired by a National Instruments' data acquisition (SCXI) system and software package in order to control the test section power; monitor flow loop test parameters (i.e., temperatures, pressures, and flow rates), and acquire boiling heat transfer data during all test runs.

3. Testing definitions and procedures

Since flow conditions leading to CHF can have wide variations, the phenomenon has been divided into two broad categories depending on the vapor quality of the bulk fluid. The first category, characterized by relatively low vapor qualities ($<\sim 0.3$), typically occurs when the cooling fluid is under high pressures and/or high mass flow rates. Under these conditions, CHF is noted for its quick transition from nucleate boiling to film boiling in response to the rapid increase in surface temperature. As a result, this category of CHF is often referred to as departure from nucleate boiling (DNB), fast burnout, or burnout of the first kind. The second category, characterized by relatively high vapor qualities ($>\sim 0.3$), occurs when the system pressure and/or the mass flow rate are relatively low. Under these conditions, the liquid film next to the heated surface develops a large dry patch that can no longer be rewetted by the moving fluid, causing a rapid increase in surface temperature. Consequently, this category of CHF is often referred to as dry-out, slow burnout, or burnout of the second kind [1–3,5,30,31]. The flow conditions encountered in this study fall under the second category of CHF, where the terms dry-out, slow burnout, or burnout of the second kind apply.

The current experimental investigation focused on two geometric factors and two flow parameters that were presumed to have a measurable affect on the CHF of the system. These factors include two main channel gap widths and flow with and without side vents. The mass flux through the test section and the input power to the heated plates varied in combination with these factors. Other parameters, such as the fluid pressure and inlet temperature, or subcooling, were not intentionally varied during test runs but were, instead, held constant at atmospheric and 20 °C, respectively. If perturbations in these values occurred, they were accounted for in the analysis of the data.

Table 1 shows the test matrix developed to organize the collection of data. The test matrix was divided into two major sections, gap widths of 1.0 mm and 2.0 mm, and two subsections, test section geometry with side vents and without side vents. Under each subsection, five separate categories are labeled for each of the major test cases. The first category is for the single phase, energy balance data used to determine how close calculated power outputs were to the measured power outputs. The second two categories, which appear in both with and without side-vents subsections, are identified by the method used to reach CHF, namely fixing the mass flux and increasing the power until CHF occurs, or fixing the power level and decreasing the flow rate until CHF occurs. The last two categories are identified for the natural circulation tests, which were only investigated with side vents in place. These two categories included natural circulation data where the down-flow of water was stopped and up-flow initiated due to natural circulation and where the initial flow of water was stopped until up-flow was initiated by natural circulation. A total of 88 separate tests were performed under the two major sections. The procedures for collecting the CHF data for the two different gap widths and test section side vent configurations are identical. The only differences occurred when test cases switched from forced convection flow to natural circulation or when the test cases used increasing power as opposed to decreasing flow conditions to approach CHF.

4. Discussion and results

In order to quantify CHF characteristics of the test section, the analysis of the data collected in this study was based on the relationships between pressure, temperature, flow rate, and electrical power input to the flow system. Other parameters, such as the cooling fluid properties, the test section material properties, and dimensionless flow parameters based on liquid–vapor phase-change physics, were also included in the analysis. A look at historically important CHF parameters and correlations form a basis for presenting and comparing the CHF results from this study. A new CHF correlation is presented that results from data collected in this study and three previous INL studies [18,29,32]. This new correlation incorporates significant improvements over past correlations because of its inclusion of conjugate heat transfer effects, accounting for the properties of the heated substrate as well as the cooling fluid.

This new correlation is valid for a water–aluminum based system where the water coolant is flowing upward through four primary flow channels and three side-flow channels (see Section 2, Experimental Apparatus, and Fig. 2). The pressure, temperature, and mass flux values for the correlated data range between 10.3 and 344 kPa, 291 and 344 K, and 9.5–110 kg m^{-2} s^{-1}, respectively. The input power was uniformly distributed over the length of the flow channels. The point at which CHF occurred was determined by a rapid increase in substrate temperature in each primary flow channel measured with embedded thermocouples. In all cases, the point of CHF simultaneously occurred at the exit of all four primary flow

Table 1
Critical heat flux test matrix

Without vents			With vents			
Energy balance fix power level (%)	Increase power fix mass flux ($kg\,m^{-2}\,s^{-1}$)	Decrease flow fix power level (%)	Increase power fix mass flux ($kg\,m^{-2}\,s^{-1}$)	Decrease flow fix power level (%)	Natural circulation	
					Down, up-flow, increase power (%)	Up-flow, increase power (%)
1.0 mm gap width (s)						
10	26	45	15	45	10	10
15	34	55	20	55	15	15
20	43	65	25	65	20	20
25	51	75	30	75	25	25
30	60	85	35	85	30	30
35	70	–	40	–	35	35
40	–	–	–	–	40	40
–	–	–	–	–	45	45
–	–	–	–	–	50	–
Energy balance calculations	Increase power fix mass flux	Decrease flow fix power level	Increase power fix mass flux	Decrease flow fix power level	Natural circulation	
					Down, up-flow increase power	Up-flow increase power
2.0 mm gap width (s)						
–	14	50	10	50	10	10
–	20	60	15	60	15	15
–	27	70	20	70	20	20
–	34	80	25	80	25	25
–	–	90	–	90	30	30
–	–	100	–	100	35	35
–	–	–	–	–	40	40
–	–	–	–	–	45	45
–	–	–	–	–	50	50
–	–	–	–	–	55	55
–	–	–	–	–	60	60

channels. This was verified with the temperature data and a visual inspection of the front two flow channels through viewing windows (see Fig. 2).

In light of the temperature and visual data collected in this study, flow instabilities caused by a multiple-channel test configuration did not have an appreciable impact on the location (one channel versus another channel) of CHF for upflow conditions. Similar conclusions were made by O'Brien and Stoots [29], whose study looked at the upward flow of water through four rectangular aluminum flow channels.

4.1. Historically important CHF parameters

Zuber [33] and Kutateladze [34] introduced a set of dimensionless parameters based on the hydraulic instabilities that cause departure from nucleate boiling (DNB). These parameters have become widely used to cast CHF correlations in dimensionless form and are defined as:

$$q^* = \frac{q}{A_h h_{fg}(\lambda \rho_g g \Delta\rho)^{1/2}} \tag{1}$$

$$G^* = \frac{G}{(\lambda \rho_g g \Delta\rho)^{1/2}} \tag{2}$$

$$\lambda = \left(\frac{\sigma}{g\Delta\rho}\right)^{1/2} \tag{3}$$

The first correlation examined by this study, that of Oh and Englert [18], was developed based on a simplified energy balance approach, where the slope and y-intercept constants of the correlation were determined by fitting a linear curve to their data. The general form of their resulting correlation and the dimensionless parameters shown in Eqs. (1)–(3) were used as the basis for recasting and comparing correlations from this and previous CHF studies. Table 2 shows the recast correlations from these previous CHF studies. Since Eq. (1) uses the heated surface area as a parameter, all recast correlations were arranged so that the dimensionless heat flux parameter takes the form $(A_h/A)q^*$. The flow channel cross-sectional area and heated area parameters shown in $(A_h/A)q^*$ are calculated as follows:

$$A = ws \tag{4}$$

$$A_h = w_h L_h \tag{5}$$

In addition, the inlet subcooling enthalpy, Δh_i, which is defined as the difference between the cooling fluid enthalpy at the saturation temperature and the inlet temperature, is used in several CHF correlations. This parameter is written as:

$$\Delta h_i = c_p(T_{sat} - T_i) \tag{6}$$

A comparison of the recast correlations shown in Table 2 with the data collected in this study and three previous

Table 2
Previous CHF correlations found to be relevant to the current study

Source	Correlation	Flow type	
Katto [9]	$\left(\frac{A_h}{A}\right)q^* = \left(We_L^{-1}\right)^{0.043}\left[1+1.043\left(We_L^{-1}\right)^{-0.043}\frac{\Delta h_i}{h_{fg}}\right]G^*, \quad We_L^{-1} = \frac{\sigma\rho_f}{G^2L}$	Up-flow, down-flow	(7)
Oh and Englert [18]	$\left(\frac{A_h}{A}\right)q^* = 0.458\left[1+\frac{\Delta h_i}{h_{fg}}\right]G^* + 2.412$	Up-flow, one-side heating	(8)
Lowdermilk et al. [35]	$\left(\frac{A_h}{A}\right)q^* = \frac{1080}{h_{fg}D_{hy}^{0.2}}\left(\frac{4A}{A_h}\right)^{-0.15}(G)^{-0.15}G^*$	Up-flow	(9)
Monde et al. [36]	$\left(\frac{A_h}{A}\right)q^* = \frac{0.16}{1+0.00067(\rho_f/\rho_g)^{0.6}}$	Up-flow	(10)
Mishima and Ishii [37]	$\left(\frac{A_h}{A}\right)q^* = \frac{\Delta h_i}{h_{fg}}G^* + 2\left(\frac{1}{1.35-0.35(\rho_g/\rho_f)^{0.5}} - 0.11\right)\left(\frac{s}{\lambda}\right)^{0.5}$	Up-flow	(11)
Mishima and Nishihara [38]	$\left(\frac{A_h}{A}\right)q^* = 0.00146\left(\frac{A_h}{A}\right)G^* + \frac{(0.725)^2(w/\lambda)^{0.5}}{[1+(\rho_g/\rho_f)^{0.25}]^2}$	Up-flow, one-side heating	(12)
Kureta and Akimoto [39]	$\left(\frac{A_h}{A}\right)q^* = \frac{C_1}{\left(\frac{A}{A_h}\right)\left(Re_L We_L^{-1}\right)^{-0.5} - C_1}\left(C_2 - \frac{\Delta h_i}{h_{fg}}\right)G^*, Re_L We_L^{-1} = \frac{\sigma}{Gv}$ $C_1 = 0.0069\left(\frac{P_h}{P_w}\right)^2 - 0.01\left(\frac{P_h}{P_w}\right) + 0.002,$ $C_2 = -0.75\left(\frac{P_h}{P_w}\right)^2 + 0.9\left(\frac{P_h}{P_w}\right) - 0.28$	Up-flow, one-side heating	(13)
Kaminaga et al. [40]	$\left(\frac{A_h}{A}\right)q^* = 0.005\left(\frac{A_h}{A}\right)G^{*0.611} + \frac{0.7(w/\lambda)^{0.5}}{[1+(\rho_g/\rho_f)^{0.25}]^2}$	Up-flow, down-flow	(14)

INL studies [18,29,32] are shown in Figs. 3a and b. The studies of Lowdermilk et al. [35] and Monde et al. [36], however, are not included in this figure because they greatly underpredict the dimensionless parameter $(A_h/A)q^*$ compared to the same parameter calculated in this and previous INL studies [18,29,32].

The results from these comparisons indicate that none of the correlations from previous studies predict well the experimental results from this study. In fact, the correlations of Katto [9], Mishima and Ishii [37], Mishima and Nishihara [38], Oh and Englert [18], and Kureta and Akimoto [39] underpredict the dimensionless critical heat flux partameter from this study, while the correlations of Mishima and Nishihara [38] and Kaminaga et al. [40] overpredict this same parameter. Three of the studies, Mishima and Ishii [37], Mishima and Nishihara [38] and Kaminaga et al. [40], show data in two separate groups consistent with the two gap widths examined in this study. These separate data groups suggest that the channel gap width is an important parameter when developing a CHF correlation.

The comparison of previous correlations with the data of Oh and Englert [18], Oh [32], and O'Brien and Stoots [29], shown in Figs. 3b, indicate similar under and overprediction trends as those seen in Fig. 3a. This comparison also shows more scatter in the data consistent with the wider range of temperatures, pressures, and flow velocities compared to those used in this study. This additional scatter in the data is evidence that the comparative correlations do not contain all of the important parameters needed to predict the CHF condition. In fact, the margin of error in their predictive capabilities (i.e., ±17% in the Oh and Englert [18] correlation) is the best indication that essential flow boiling parameters are not incorporated into the correlation.

4.2. New CHF correlation development

Several CHF parameters from Table 2 are important to the development of a new CHF correlation because they account for trends in the data from this and previous INL studies [18,29,32] (see Figs. 3a and b). These parameters, which are in addition to those presented in Eqs. (1)–(3), include the inverse Weber number, the ratio of subcooling to vaporization enthalpies, the ratio of liquid to gas densities of the fluid, and the ratio of heated to cross-sectional flow areas. Several parameters that account for conjugate heat transfer effects in a flow boiling system have not been included in previous correlations. These parameters are generally embedded in the thermodynamic properties of the substrate material and its interaction with the cooling fluid. The Biot number and a combination of the thermal conductivity, the density, and the specific heat of the substrate and cooling fluid are some key parameters that affect conjugate heat transfer of boiling systems. The inclusion of these parameters in a new CHF correlation provides for a more accurate and robust representation of CHF data.

Determining the form of a new CHF correlation using the parameters identified above was an iterative process that involved fitting a trend line to the data from this and previous INL studies and then refining its fit by manipulating the parameters used to plot the data. Several attempts were made at finding the right combination of flow parameters that best described the characteristics of flow boiling CHF. In many instances, a trial and error approach was used as part of the iterative process. Nevertheless, careful thought was taken to understand the general effects a new parameter would have on correlating the data before it was included in the new correlation.

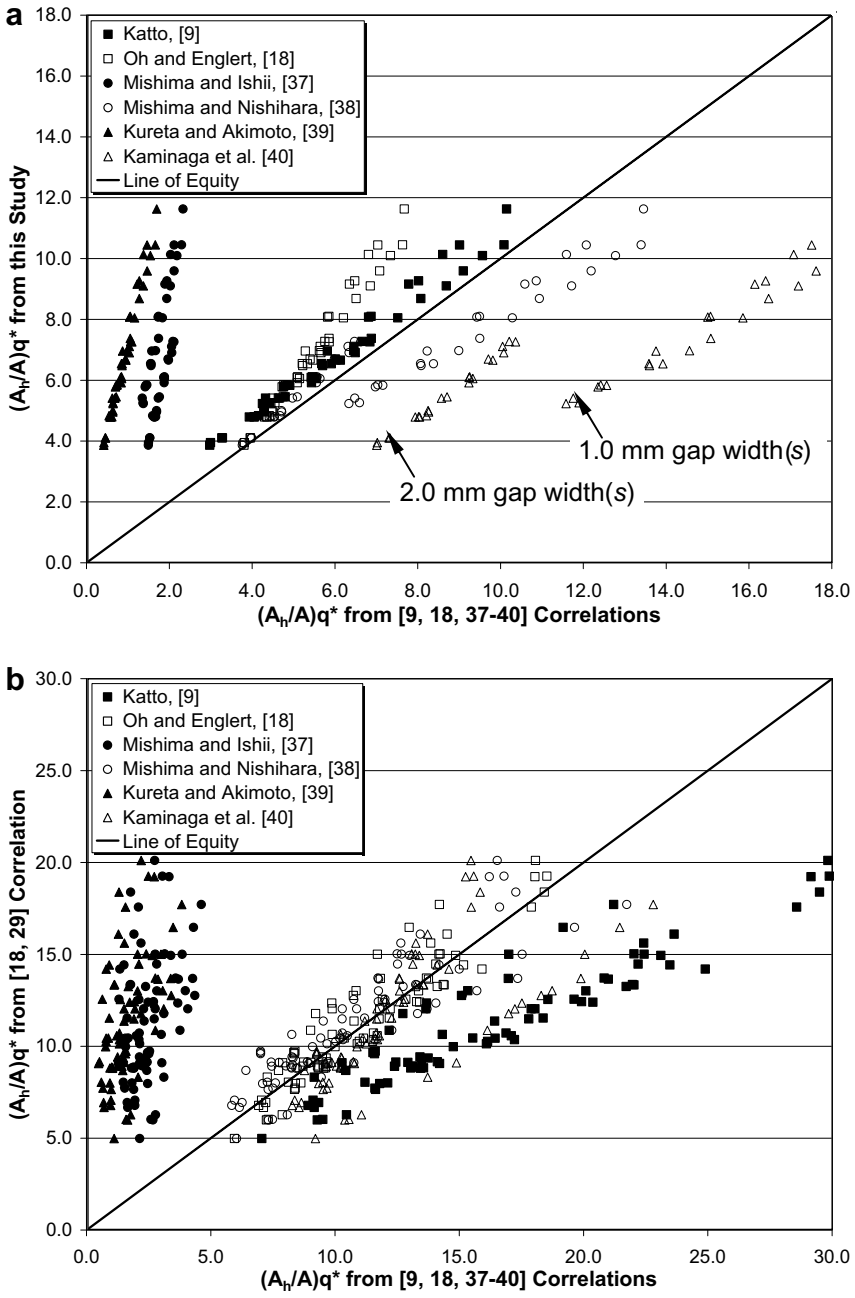

Fig. 3. Comparison of calculated $(A_h/A)q^*$ (abscissa) from previous CHF studies with (a) calculated $(A_h/A)q^*$ (ordinate) from this study and (b) calculated $(A_h/A)q^*$ (ordinate) from Oh and Englert [18] and O'Brien and Stoots [29].

For brevity, only the major iterations along the path to producing the final CHF correlation are discussed in the following sections.

4.3. First correlation iteration

Because of its accuracy in predicting the data from this study, as shown in Fig. 3a, the correlation of Katto [9] (see Table 2) was used as the basis for a new correlation. More specifically, the contribution of the inverse Weber number (modified to be based on hydraulic diameter) from this correlation was felt to be important since it captured an additional degree of mass flow variability through system. However, only the first Weber number term from Katto's [9] correlation was included in the iterative process since the second Weber number term was observed to cause more scatter in the data when included. Subsequently, a modified form of the Biot number was added to the correlation in order to account for some of the conjugate heat transfer effects found to be important to a flow boiling system. A first cut in this iterative process produced the following correlation:

$$\left(\frac{A_h}{A}\right)q^* = 0.121\left(We_D^{-1}\right)^{0.2}(Bi)\left[1+\frac{\Delta h_i}{h_{fg}}\right]G^* + 4.459 \qquad (15)$$

where the power, slope, and y-intercept constants were determined through a linear fit to the data. The modified form of the inverse Weber and Biot numbers are, respectively,

$$We_{\mathrm{D}}^{-1} = \frac{\sigma \rho_{\mathrm{f}}}{G^2 D_{\mathrm{hy}}} \tag{16}$$

$$Bi = \frac{hL_{\mathrm{c}}}{k_{\mathrm{m}}} \tag{17}$$

Two variables in the modified Biot number, the heat transfer coefficient, h, and the characteristic length, L_{c}, required additional calculations before their insertion into Eq. (17). The heat transfer coefficient was calculated using Shah's [41] correlation, which was specifically developed to model two-phase flow systems, where many of the parameters are the same as those affecting CHF. Shah's [41] correlation was chosen for use in this study, as opposed to the more widely used Chen [42] correlation, because of its ability to better predict the heat transfer coefficient in rectangular channels [29].

The second variable, the characteristic length, is composed of the total volume of the substrate material, V, and the total heated area of the flow channel, A_{h}. The ratio of volume to heated surface area is often used as the characteristic length in the lumped capacitance method for determining the combined convective and conductive heat transfer [43]. Since these two variables are constant for any given test section configuration, the characteristic length is unique to a particular test section and data set, so long as the cooling fluid remains the same. The equation describing the relationship between substrate volume, flow channel heated area, and the characteristic length is given by

$$L_{\mathrm{c}} = \frac{V}{A_{\mathrm{h}}} \tag{18}$$

A system's ability to absorb energy, as discussed previously, can have a significant effect on the resulting CHF data. Thus, the total volume of the substrate material is important to a CHF correlation because it accounts for the mass of a system capable of storing heat during testing. Based on the literature search performed for this study, the total volume of the substrate material has never been used to quantify the energy storage capacity of a system, which may be one of the primary sources of inconsistencies between data from different CHF studies. Accounting for the mass of the test section allows for inclusion of conjugate heat transfer effects presumed to exist in a flow boiling system.

The heated area variable is a useful quantity when trying to identify the heat flux capacity of a particular test section. The inclusion of this variable in a CHF correlation can help quantify this effect across different heating configurations for different test sections. At first glance, it would appear that this variable is already included in most correlations in the $(A_{\mathrm{h}}/A)q^*$ parameter. However, since the dimensionless CHF parameter, q^*, already contains the heated area in its denominator (see Eq. (1)), the direct influence of the heated area is eliminated from the correlation. Including the heated area in the characteristic length is one way of reasserting its influence on the CHF condition. The results of applying this first-cut correlation expressed in Eq. (15) to the data from this and previous INL studies [18,29,32] are shown in Fig. 4.

The overall accuracy of this new correlation is shown by the error lines in Fig. 4 to be ±22%. The success of this new

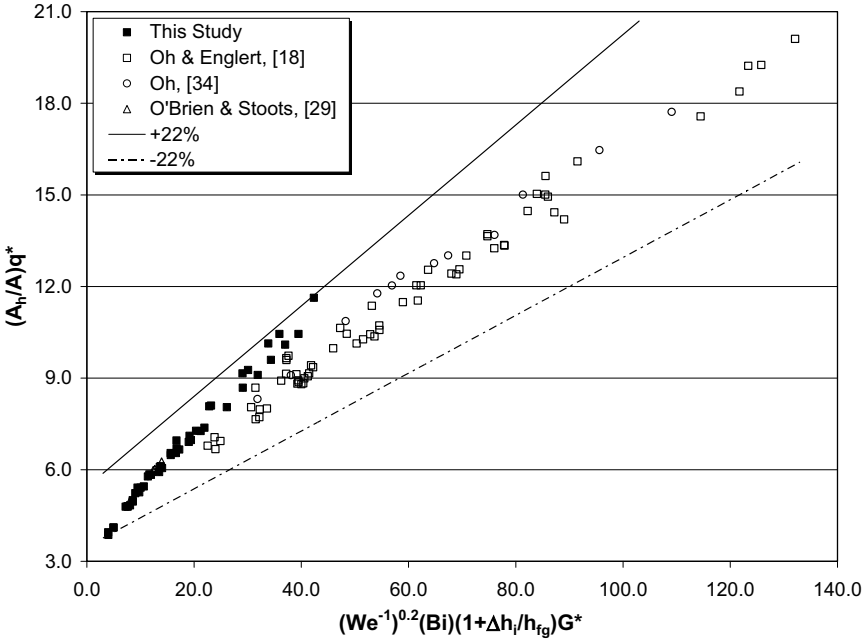

Fig. 4. A plot of all 126 data points from this study and previous INL studies [18,29,32] based on a first-cut correlation shown in Eq. (15). The ±22% error lines bracket the data according to the accuracy of this correlation.

correlation in collapsing data from this and previous INL studies [18,29,32] into a relatively tight group indicates that the chosen parameters are having a positive effect on correlating the data. However, the overall accuracy of this new correlation indicates that certain characteristics of the flow are not adequately captured. In fact, the different relative slopes of the data sets are a good indication that additional characteristics of the flow need to be captured.

4.4. Second correlation iteration

Further efforts to improve the correlation led to the inclusion of the liquid-to-gas densities ratio of the cooling fluid, given by

$$1+\left(\frac{\rho_g}{\rho_f}\right)^{0.25} \tag{19}$$

This quantity accounts for liquid and vapor interactions, localized bubble dynamics, and overall buoyancy effects on the system. Including this parameter should help to implicitly capture the varying pressure conditions from the four different studies used to develop the correlation. Many of the data from these studies included test section pressures that were significantly below or above atmospheric. Furthermore, the density ratio parameter appears in several of the correlations used as a basis for developing this new correlation (see Table 2) [36–38,40]. In most cases, this parameter appears in the y-intercept term, which is used to quantify CHF when flow through the channel is zero. In the case of this study, however, this parameter is included with the slope terms because of its influence on the amount of heat that can be locally conducted away from the heated surface as a function of bubble formation and departure at the solid liquid interface.

The initial form of the revised correlation started with the density parameter as it is seen in the correlation of Mishima and Nishihara [38], and Kaminaga et al. [40]. After some manipulation to optimize the fit of the trend line, the final form of the revised correlation was produced and is given as

$$\left(\frac{A_h}{A}\right)q^* = 0.145\left[1+\left(\frac{\rho_g}{\rho_f}\right)^{0.25}\right]^{6.4}\left(We_D^{-1}\right)^{0.4}(Bi)\left[1+\frac{\Delta h_i}{h_{fg}}\right]G^* + 2.579 \tag{20}$$

This revised correlation is a refinement of the first correlation based on the addition of the liquid-to-gas densities ratio. It is important to point out that the values of the exponents on each of the terms in the correlation, including those identified in previous iterations, change from iteration to iteration in order to achieve the best possible fit of the trend line. A plot of this revised correlation and its affect on the data from this and previous INL studies [18,29,32] is shown in Fig. 5.

A comparison of this correlation, Fig. 5, with the first attempt at a new correlation, Fig. 4, shows a significant improvement in the grouping of the data. The revised correlation, through the addition of the density parameter, has aligned the slopes and improved the linear grouping of the different data sets. The error bands around the data are now +19% and −11%, which constitutes over a 30% reduction in the maximum error between the two correlations. In

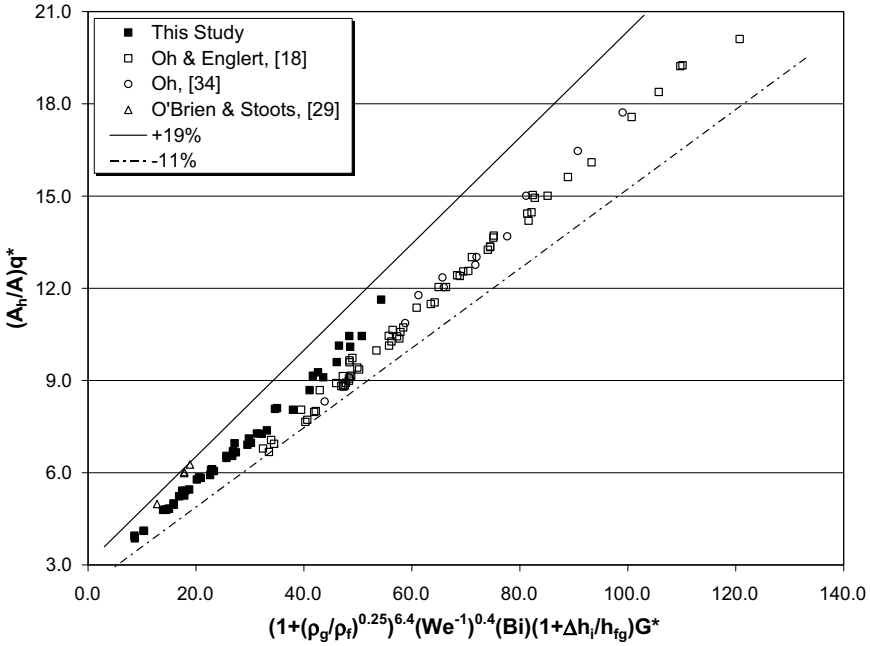

Fig. 5. A plot of all 126 data points from this study and previous INL studies [18,29,32] based on a first-cut correlation shown in Eq. (20). The +19/−11% error lines bracket the data according to the accuracy of this correlation.

general, this could be considered a reasonably good correlation when taking into account the wide range of flow parameters and test section geometries used in the studies that produced the data. However, this correlation is still limited to data from an aluminum/water flow system and does not account for different heated substrates or cooling fluids.

4.5. Final correlation iteration

The final iteration for developing a new CHF correlation included a parameter (see Eq. (21)) that accounts for the thermal interactions between the cooling fluid and the heated substrate. This parameter – the square root ratio of fluid to substrate thermal products – is commonly used in transient heat transfer analyses where the depth and effectiveness of heat penetration into both the fluid and heating material are quantified. The primary purpose for including this parameter is to account for interactions between the heated substrate and the cooling fluid. Its inclusion will, in general, allow the final correlation to be more robust and universal in nature by providing a way to predict the behavior of a CHF system using different cooling fluids and different heated substrate materials. This level of flexibility does not exist in current CHF correlations.

$$\left(\frac{k_f \rho_f c_{p,f}}{k_m \rho_m c_{p,m}}\right)^{0.5} \tag{21}$$

A new formulation for the calculation of the heat transfer coefficient, h, was also included in this final CHF correlation. This new formulation replaced Shah's [41] formulation in order to update the basis of the calculations with more recent experimental data and advanced heat transfer knowledge. The new heat transfer coefficient is used in the calculation of the Biot number, which is critical in accurately assessing the heat transfer interaction between the cooling fluid and the heated substrate.

The foundation of this new formulation is the work of Tran et al. [44], who observed that the dominant mechanism in boiling heat transfer is nucleation rather than convection. Thus, their correlation for the heat transfer coefficient replaced the typically used Reynolds number with the Weber number to account for the dominant surface tension effects over the viscous effects. Yu et al. [45] confirmed this relationship and modified Tran et al.'s [44] correlation to fit their experimental data. In a similar fashion, this study confirmed the trends found in the study of Yu et al. [45] by testing the formula for the heat transfer coefficient in the new CHF correlation. Slight modifications to the exponents on each term and the basis of the Weber number were made in order to obtain the best fit to the CHF data. The new heat transfer formulation used in the development of the final CHF correlation is given as

$$h = 6.4 \times 10^6 (Bo^{2.1} We_D)^{0.28} \left(\frac{\rho_g}{\rho_f}\right)^{0.21} \tag{22}$$

where the Weber number is the inverse of Eq. (16), and the Boiling number is given by

$$Bo = \frac{q''_{chf}}{G h_{fg}} \tag{23}$$

The characteristic length used in the modified Biot number was also revised to include the flow channel gap width, s, instead of the heated area, A_h. This change was made because the data showed discrepancies that could be directly tied to the different gap with test cases. This is reasonable since the purpose of the Biot number, as used in this study, is to relate the heat transfer characteristics of the fluid and the substrate over a characteristic length that is significant to boiling flows in rectangular channels. Thus, the modified Biot number in this study helps quantify the conjugate heat transfer that occurs in this boiling system. The equation describing this new characteristic length relationship is given by

$$L_c = \sqrt{\frac{V}{s}} \tag{24}$$

The gap width variable is somewhat unique to flow through rectangular or annular channels and is seen in Fig. 3a and b to be important because it can possibly account for the splitting of the data due to different gap-width test cases. This variable seems to have had limited use in previous CHF correlations, such as that by Mishima and Ishii [37]. Nevertheless, the data from this study has shown that the gap-width variable is important to the development of a more complete CHF correlation.

Incorporating the changes mentioned above produced the final CHF correlation that describes the conditions for two-phase forced convection flow in long, thin rectangular channels. This new correlation was applied to the data collected from this study and three previous INL studies [18,29,32]. The geometry and flow conditions of these studies varied over a relatively large range, including the magnitude of the mass flux, the test section pressure, the inlet temperature, the cross-sectional flow geometry, the length of the heated channel, the side-vent cross-flow channels, and the single and multiple flow channel configuration. Combined, these studies produced 126 CHF data points, which were included in the development of this new CHF correlation. The final form of the new CHF correlation is

$$\left(\frac{A_h}{A}\right) q^* = 3.9 \left(\frac{k_f \rho_f c_{p,f}}{k_m \rho_m c_{p,m}}\right)^{0.5} \left[1 + \left(\frac{\rho_g}{\rho_f}\right)^{0.1}\right]^{-6.7} \left(We_D^{-1}\right)^{0.33} \times (Bi) \left(1 + \frac{\Delta h_i}{h_{fg}}\right) G^* + 0.018 \tag{25}$$

where again the slope and y-intercept constants were determined from a linear curve fit to the 126 data points used to develop the correlation. A plot of the correlated data is shown in Fig. 6.

The significance of this new correlation is that it accounts for the properties of the heated substrate and the interaction between the substrate and the cooling fluid

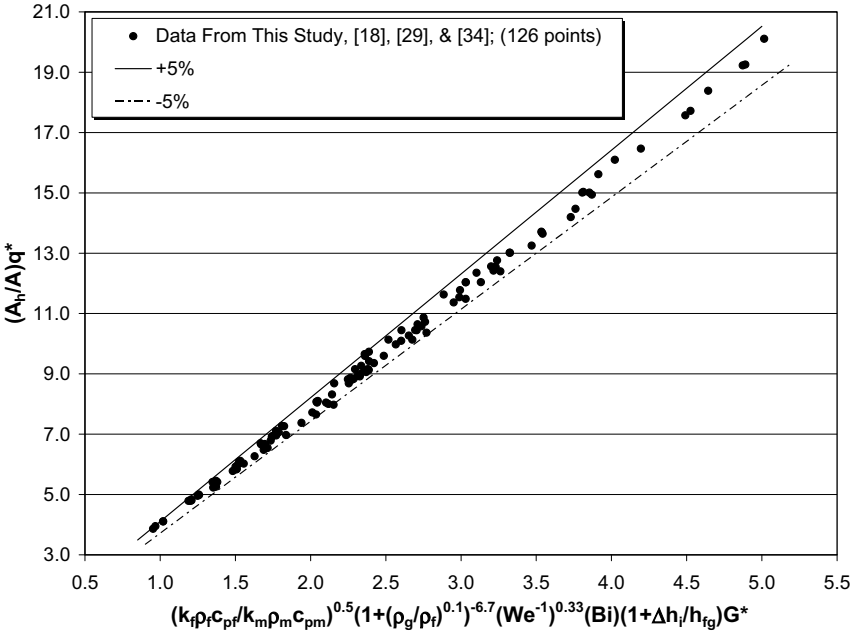

Fig. 6. Final up-flow CHF correlation for data having a ±5% correlation error.

Table 3
New CHF correlation and supporting equations

New CHF correlation	
$\left(\frac{A_h}{A}\right)q^* = 3.9\left(\frac{k_f\rho_f c_{p,f}}{k_m\rho_m c_{p,m}}\right)^{0.5}\left[1+\left(\frac{\rho_g}{\rho_f}\right)^{0.1}\right]^{-6.7}\left(We_D^{-1}\right)^{0.33}(Bi)\left(1+\frac{\Delta h_i}{h_{fg}}\right)G^* + 0.018$	Eq. (25)
Supporting equations	
$q^* = \frac{q''_{chf}}{h_{fg}(\lambda\rho_g g\Delta\rho)^{1/2}}, \quad G^* = \frac{G}{(\lambda\rho_g g\Delta\rho)^{1/2}}, \quad \lambda = \left(\frac{\sigma}{g\Delta\rho}\right)^{1/2}$	Eq. (1) Eq. (2) Eq. (3)
$We_D^{-1} = \frac{\sigma\rho_f}{G^2 D_{hy}}, \quad Bi = \frac{hL_c}{k_m}, \quad L_c = \sqrt{\frac{V}{s}}$	Eq. (16) Eq. (17) Eq. (24)
$h = 6.4\times10^6(Bo^{2.1}We_D)^{0.28}\left(\frac{\rho_g}{\rho_f}\right)^{0.21}, \quad Bo = \frac{q''_{chf}}{Gh_{fg}}$	Eq. (22) Eq. (23)

that have not previously been included in CHF correlations. Accounting for the heated substrate contributions to the boiling heat transfer and CHF of the system resulted in a correlation that is able to predict the CHF characteristics of four flow boiling studies to within ±5% (mean CHF values) or ±8.5% with uncertainties (95% confidence). This new correlation blends macroscopic operational parameters and microscopic fluid/surface parameters in order to capture a larger range of important heat transfer characteristics. A summary of the final correlation and its respective parameters is given in Table 3.

4.6. CHF data uncertainties

Estimated uncertainties in the measured and calculated values used to develop the new CHF correlation quantify the difference between the true value and reported value of the data collected during testing. Every attempt was made to eliminate recognized bias errors through calibration of the measurement equipment. Thus, the only errors quantified through this analysis are the random errors associated with signal noise or unmeasured system losses (i.e., resistance, friction, radiation cooling, etc.). In addition, some errors occur as a result of machining tolerances and data acquisition limitations such as sampling frequencies.

The uncertainty values used in the analysis are based on a single-sample data set and are derived from the macroscopic and microscopic flow parameters acquired during testing, reported from equipment literature, and determined from calibration. The analytical approach used to determine uncertainties applies the root-sum-square (RSS) method [46]. Table 4 identifies the maximum, estimated experimental uncertainties for all of the major measured and calculated parameters used in the new CHF correlation. Fig. 7 shows the CHF data from this and previous INL studies [18,29,32] plotted according to the new correlation. The ±8.5% error bars include the uncertainties in the results from this study.

Table 4
Estimated experimental uncertainties

Quantity	Symbol	Units	Maximum uncertainty
Pressure	P	Pa	±0.0025%
Temperature	T	K	±0.75%
Volume flow rate	$\dot{Q}$	$m^3\ s^{-1}$	±0.05%
Input power	q	W	±0.318%
Test section aluminum volume	V	m^3	±0.10%
Mass flow rate	$\dot{m}$	$kg\ s^{-1}$	$\pm 1.8 \times 10^{-6}$
Mass flux	G	$kg\ m^{-2}\ s^{-1}$	$\pm 3.8 \times 10^{-2}$
Critical heat flux	q''_{chf}	$W\ m^{-2}$	±4.9
Cross-sectional area	A	m^2	$\pm 7.3 \times 10^{-8}$
Heated surface area	A_h	m^2	$\pm 2.7 \times 10^{-6}$
Hydraulic-equivalent diameter	D_{hy}	m	$\pm 1.6 \times 10^{-6}$
Taylor wave length	λ	m	$\pm 4.4 \times 10^{-8}$
Heat transfer coefficient	h	$W\ m^{-2}\ K^{-1}$	±7.3
Characteristic length	L_c	m	$\pm 1.5 \times 10^{-3}$
Dimensionless critical heat flux	q^*	–	$\pm 2.8 \times 10^{-6}$
Dimensionless mass flux	G^*	–	$\pm 9.8 \times 10^{-3}$
Inverse Weber number	We_D^{-1}	–	±0.32
Weber number	We_D	–	$\pm 1.1 \times 10^{-4}$
Boiling number	Bo	–	$\pm 2.1 \times 10^{-6}$
Biot number	Bi	–	±0.13
Enthalpy ratio	$(1 + \Delta h_i/h_{fg})$	–	$\pm 5.4 \times 10^{-6}$
Density ratio	See Eq. (19)	–	$\pm 1.7 \times 10^{-6}$
Thermal product ratio	See Eq. (21)	–	$\pm 1.4 \times 10^{-6}$
Correlation uncertainties			
Ordinate of the correlation	$(A_h/A)q^*$	–	$\pm 8.8 \times 10^{-3}$
Abscissa of the correlation	See Eq. (25)	–	±0.15

4.7. Final discussion

The CHF results show very little difference between test cases with and test cases without side-vent cross-flow. Observations of the flow through the side channels indicated that the level and severity of dryout was the same as that observed in the main flow channels. Since the side channels did not maintain a flow of single-phase liquid during the system's approach to CHF, there was no additional cooling fluid passing over the heated plates as anticipated. Thus, all CHF data points could be correlated without respect to whether the flow was with or without side-vents. It is possible that a strong link to the conductivity of the heater plate material, which allowed enough heat to flow into the side channel fluid removing its ability to add additional cooling, is the primary reason no differences were measured between the two types of flow.

Comparing the mass of the heated test section from this study with previous experimental studies shows a significant difference in the total amount of material used to fabricate the flow channels. This difference in mass between various studies is a significant reason boiling flow patterns, heat transfer mechanisms, and CHF values are different. In fact, the inter-related heat transfer properties of the cooling fluid and the heated substrate, such as the thermal product and conductivity, are a fundamental cause of discrepancies in reported data. These relationships form the basis of conjugate heat transfer and its effects on the CHF condition and the flow patterns leading to burnout. In studies where the cooling fluid and heated substrate material are the same, differences in the heat transfer characteristics of the system and the final CHF are based on the system's thermal mass. It is the use of this volume in the Biot number of the newly developed CHF correlation (see Eq. (25) and Fig. 6) that helps correlate the results of these studies with a very tight error band of ±5%. A comparison between Figs. 4 and 6 shows the effects of this parameter on the overall correlation of the data.

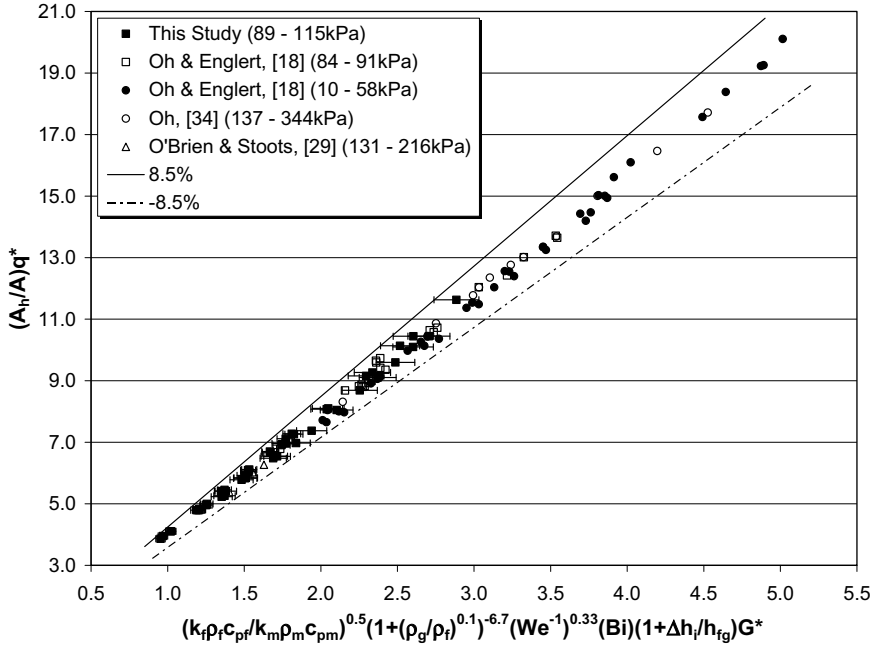

Fig. 7. Final up-flow CHF data by contributing study showing this study's uncertainty and a ±8.5% correlation error.

The thermal products of the fluid and heated substrate also capture conjugate heat transfer effects are captured on the CHF condition. Through the inclusion of Eq. (21) in the new CHF correlation, conjugate heat transfer effects are captured for studies where the cooling fluid and/or the heated substrate are not the same. This parameter provides for a much wider application of the new CHF correlation given in Eq. (25).

5. Conclusions

Experimentally measured CHF results from the present study were not well-predicted by existing CHF correlations developed for atmospheric or lower pressure systems under low-flow conditions in narrow, rectangular, aluminum channels. These correlations are limited by the number and types of parameters used to describe the CHF condition and tend to over- or under-predict the results from this study. Specifically, existing correlations do not account for the conjugate heat transfer effects between the heated substrate material and the cooling fluid. This study shows that these effects can significantly influence the energy storage capacity of the test section, the response time of the system during heat-flux increases, and, ultimately, the point at which CHF is reached. In addition, conjugate heat transfer effects are linked to differences between steady-state and transient flow conditions, which affect the stability of two-phase flows.

Through a search of literature and a comparison of previous CHF results, this work has contributed to the study of boiling heat transfer and CHF for the purpose of improving the heat transfer characteristics of high heat-flux systems, such as nuclear reactors. The primary product of this research is the development of a new CHF correlation based on the findings of previous studies and an applied understanding of conjugate heat transfer effects captured in the Biot number and the ratio of fluid and heated substrate thermal products. This new correlation relates the results of this study and the studies of Oh and Englert [18], Oh [34], and O'Brien and Stoots [29] with an error band of $\pm 5\%$ (mean CHF values) or $\pm 8.5\%$ with uncertainties (95% confidence). Eq. (25) and Fig. 6 show the mathematical and graphical representations of this new correlation.

References

[1] A.E. Bergles, Burnout in boiling heat transfer. Part II: Subcooled and low-quality forced-convection systems, Nucl. Safety 18 (2) (1977) 154–167.

[2] R.D. Boyd, Review of subcooled flow boiling critical heat flux (CHF) and its application to fusion systems. Part I: fundamentals of CHF, American Society of Mechanical Engineers, Heat Transfer Division, (Publication) HTD 24, 1983, pp. 19–30.

[3] R.D. Boyd, Subcooled flow boiling critical heat flux (CHF) and its application to fusion energy components. Part I: A review of fundamentals of CHF and related data base, Fusion Technol. 7 (1) (1985) 7–30.

[4] R.T. Pagh, Annular Geometry Critical Heat Flux Correlation Generation, Pacific Northwest National Laboratory, Richland, Washington, DOE, 1999 (DE-AC06-76RLO 1830, pp. 1–20).

[5] L. Bernath, A theory of local-boiling burnout and its application to existing data, Chem. Eng. Prog. Symp. Ser. 56 (30) (1960) 95–116.

[6] A.E. Bergles, W.M. Rohsenow, The determination of forced-convection surface-boiling heat transfer, J. Heat Transfer 86 (8) (1964) 365–372.

[7] D.C. Groeneveld, S.C. Cheng, T. Doan, 1986 AECL-UO critical heat flux lookup table, Heat Transfer Eng. 7 (1) (1986) 46–62.

[8] K.E. Gungor, R.H.S. Winterton, A general correlation for flow boiling in tubes and annuli, Int. J. Heat Mass Transfer 29 (3) (1986) 351–358.

[9] Y. Katto, General features of CHF of forced convection boiling in uniformly heated rectangular channels, Int. J. Heat Mass Transfer 24 (8) (1981) 1413–1419.

[10] V.V. Klimenko, A general correlation for two-phase forced flow heat transfer, Int. J. Heat Mass Transfer 31 (3) (1988) 541–552.

[11] S.G. Kandlikar, A general correlation for saturated two-phase flow boiling heat transfer inside horizontal and vertical tubes, J. Heat Transfer 112 (2) (1990) 219–228.

[12] M. Kaminaga, K. Yamamoto, Y. Sudo, Improvement of critical heat flux correlation for research reactors using plate-type fuel, J. Nucl. Sci. Technol. 35 (12) (1998) 943–951.

[13] M.W. Croft, Advanced test reactor burnout heat transfer tests, United States Atomic Energy Commission Report, IDO-24465, Babcock & Wilcox Company, January 1964.

[14] E.D. Waters, Heat transfer experiments for the advanced test reactor, United States Atomic Energy Commission Report, BNWL-216, Battelle-Northwest, May 1966.

[15] W.R. Gambill, Burnout in boiling heat transfer. Part II: Subcooled forced-convection systems, Nucl. Safety 9 (9) (1968) 467–480.

[16] K. Mishima, H. Nishihara, I. Michiyoshi, Boiling burnout and flow instabilities for water flowing in a round tube under atmospheric pressure, Int. J. Heat Mass Transfer 28 (6) (1985) 1115–1129.

[17] L.Y. Cheng, P.R. Tichler, Analysis of Flow Reversal Test, Brookhaven National Laboratory, Upton, New York, 1991.

[18] C.H. Oh, S.B. Englert, Critical heat flux for low flow boiling in vertical uniformly heated thin rectangular channels, Int. J. Heat Mass Transfer 36 (2) (1993) 325–335.

[19] Y. Sudo, K. Miyata, H. Ikawa, M. Kaminaga, M. Ohkawara, Experimental study of differences in DNB heat flux between up-flow and down-flow in vertical rectangular channel, J. Nucl. Sci. Technol. 22 (8) (1985) 604–618.

[20] Y. Sudo, K. Miyata, H. Ikawa, M. Ohkawara, M. Kaminaga, Experimental study of differences in single-phase force-convection heat transfer characteristics between up-flow and down-flow for narrow rectangular channel, J. Nucl. Sci. Technol. 22 (3) (1985) 202–212.

[21] Y. Sudo, M. Kaminaga, A new CHF correlation scheme proposed for vertical rectangular channels heated from both sides in nuclear research reactors, J. Heat Transfer 115 (5) (1993) 426–434.

[22] R.G. Ambrosek, J.L. Durney, Review of critical heat flux test and correlations for ATR, Memo AMB-14-87, Idaho National Engineering and Environmental Laboratory, Idaho Falls, ID, December 1987.

[23] F. Tachibana, M. Akiyama, H. Kawamura, Non-hydrodynamic aspects of pool boiling burnout, J. Nucl. Sci. Technol. 4 (3) (1967) 121–130.

[24] K. Mishima, H. Nishihara, The effects of flow direction and magnitude on CHF for low pressure water in thin rectangular channels, Nucl. Eng. Des. 86 (5) (1985) 165–181.

[25] M. Murase, H. Suzuki, T. Matsumoto, M. Naitoh, Countercurrent gas–liquid flow in boiling channels, J. Nucl. Sci. Technol. 23 (6) (1986) 487–502.

[26] H. Suzuki, S. Hatamiya, M. Murase, Parallel channel effects under BWR LOCA conditions, Nucl. Eng. Des. 109 (11) (1988) 399–405.

[27] J.A. Boure, A.E. Bergles, L.S. Tong, Review of two-phase flow instability, Nucl Eng. Des. 25 (7) (1973) 165–192.

[28] M.Z. Podowski, R.T. Lahey Jr., A. Clausse, Modeling and analysis of channel-to-channel instabilities in boiling systems, Chem. Eng. Commun. 93 (1) (1990) 75–92.
[29] J.E. O'Brien, C.M. Stoots, Parallel channel effects for low flow boiling in vertical thin rectangular channels, in: Proceedings of the Sixth AIAA/ASME Thermophysics and Heat Transfer Conference, American Society of Mechanical Engineers, Colorado Springs, CO, 1994, pp. 81–91.
[30] A.E. Bergles, Burnout in boiling heat transfer. Part III: High-quality forced-convection systems, Nucl. Safety 20 (6) (1979) 671–689.
[31] M.S. El-Genk, S.J. Haynes, S. Kim, Experimental studies of critical heat flux for low flow of water in vertical annuli at near atmospheric pressure, Int. J. Heat Mass Transfer 31 (1) (1988) 2291–2304.
[32] C.H. Oh, High pressure CHF data, INEL Interoffice Correspondence, CHO-08-93, Idaho Falls, ID, October, 1993.
[33] N. Zuber, Hydrodynamic aspects of boiling heat transfer, PhD thesis, University of California Los Angeles, Los Angeles, CA, 1959.
[34] S.S. Kutateladze, Heat transfer in condensation and boiling, Atomic Energy Commision – translation, AEC-tr-3770, 1959.
[35] W.H. Lowdermilk, C.D. Lanzo, B.L. Siegel, Investigation of boiling burnout and flow instability of water flowing in tubes, NACA-Technical Note 4382, September, 1958.
[36] M. Monde, H. Kusuda, H. Uehara, Critical heat flux during natural convective boiling in vertical rectangular channels submerged in saturated liquid, J. Heat Transfer 104 (5) (1982) 300–303.
[37] K. Mishima, M. Ishii, Flow regime transition criteria for upward two-phase flow in vertical tubes, Int. J. Heat Mass Transfer 27 (1) (1984) 723–737.
[38] K. Mishima, H. Nishihara, The effects of flow direction and magnitude on CHF for low pressure water in thin rectangular channels, Nucl. Eng. Des. 86 (5) (1985) 165–181.
[39] M. Kureta, H. Akimoto, Critical heat flux correlation for subcooled boiling flow in narrow channels, Int. J. Heat Mass Transfer 45 (9) (2002) 4107–4115.
[40] M. Kaminaga, Y. Sudo, Y. Murayama, Experimental study of the critical heat flux in a narrow vertical rectangular channel, Heat Transfer – Jpn. Res. 20 (1) (1991) 72–85.
[41] M.M. Shah, Chart correlation for saturated boiling heat transfer: Equations and further study, ASHRAE – Am. Soc. Heat., Refrig., Air Conditioning Eng. Trans. 88 (1) (1982) 185–196.
[42] J.C. Chen, Correlation for boiling heat transfer to saturated fluids in convective flow, Ind. Eng. Proc. Des. Dev. 5 (7) (1966) 322–339.
[43] F.P. Incropera, D.P. DeWitt, Fundamentals of Heat and Mass Transfer, fourth ed., John Wiley & Sons, New York, 1996, pp. 212–221.
[44] T.N. Tran, M.W. Wambsganss, D.M. France, Small circular- and rectangular-channel boiling with two refrigerants, Int. J. Multiphase Flow 22 (6) (1996) 485–498.
[45] W. Yu, D.M. France, M.W. Wambsganss, J.R. Hull, Two-phase pressure drop, boiling heat transfer, and critical heat flux to water in small-diameter horizontal tube, Int. J. Multiphase Flow 28 (6) (2002) 927–941.
[46] R.J. Moffat, Describing the uncertainties in experimental results, Exp Therm Fluid Sci 1 (1) (1988) 3–17.